Quantitative study of bundle size effect on thermal conductivity of single-walled carbon nanotubes

Ya Feng[1], *Taiki Inoue*[1], *Hua An*[1], *Rong Xiang*[1], *Shohei Chiashi*[1], *Shigeo Maruyama*[1, 2, *]

[1]Department of Mechanical Engineering, The University of Tokyo, Tokyo 113-8656, Japan

[2]Energy NanoEngineering Lab., National Institute of Advanced Industrial Science and Technology, Tsukuba 305-8564, Japan

This manuscript was accepted by Appl. Phys. Lett. Click here to see the version of record.

ABSTRACT: Compared with isolated single-walled carbon nanotubes (SWNTs), thermal conductivity is greatly impeded in SWNT bundles; however, measurement of the bundle size effect is difficult. In this study, the number of SWNTs in a bundle was determined based on the transferred horizontally aligned SWNTs on a suspended micro thermometer to quantitatively study the effect of the bundle size on thermal conductivity. Increasing bundle size significantly degraded the thermal conductivity. For isolated SWNTs, thermal conductivity was approximately 5000±1000 $Wm^{-1}K^{-1}$ at room temperature, three times larger than that of the four-SWNT bundle. The logarithmical deterioration of thermal conductivity resulting from increased bundle size can be attributed to the increased scattering rate with neighboring SWNTs based on the kinetic theory.

KEYWORDS: single-walled carbon nanotube, bundle size effect, horizontally aligned, thermal conductivity

Carbon nanotubes (CNTs) have been widely used and examined for electronic applications, such as field-effect transistors,[1, 2] but the working stability and durability of CNT electronics are highly dependent on the thermal behavior of CNTs. Therefore, understanding the relation between the thermal transport properties of individual CNTs and their nanoscale structure will be useful for the future design of CNT electronics. Thermal conductivity of suspended monolayer graphene is one order of magnitude larger than that of supported monolayer graphene, due to the suppression of flexural phonons by interface scatterings in the latter.[3, 4] The thermal conductivity of suspended multi-layer graphene is proved to be much lower than that of monolayer graphene because of inter-planar phonon-phonon interactions that similarly suppress flexural acoustic modes transport.[5]

This manuscript was accepted by Appl. Phys. Lett. Click here to see the version of record.

When comparing isolated single-walled carbon nanotubes (SWNTs) with bundled SWNTs, previous studies[6, 7] show a similar decrease in the thermal conductivity of the latter; however, computational simulation[8] indicates only a slight difference in the conductivity values of isolated and bundled SWNTs. On account of the difficulty of sample preparation, the bundle size of SWNTs can hardly be controlled and determined; therefore, the relation between the thermal conductivity and the bundle size of SWNTs has seldom been studied to account for inter-tube interactions. In the present work, such a quantitative study was achieved by employing an experimental design allowed for the bundle size to be selectively chosen based on the transferred horizontally aligned SWNTs.

To study the thermal properties of individual SWNTs, suspended platinum resistance thermometers[6] were fabricated; the horizontally aligned SWNTs[9] (HA-SWNT) were grown on a crystal quartz substrate and then transferred onto the micro thermometers using poly(methyl methacrylate) (PMMA).[10] During the decomposition of PMMA by annealing at 400 °C for several hours, some SWNTs converged and formed ribbon-like bundles[11] over the gap between two thermometers, but the supported fractions of SWNTs on the thermometers remained well-aligned and dispersed. This substantially increased the overlapped area of supported SWNTs on substrate, making thermal boundary resistance (TBR) negligible in the present work. The substrate-induced alignment of SWNTs highly suppresses bundle formation during growth,[12] especially when the SWNT density is low by adjusting the growth conditions, as we did in this study.[9] The ready-for-thermal-measurement samples were examined using scanning electron microscope (SEM) and transmission electron microscope (TEM). Both examinations confirmed that the number of SWNTs in a bundle could be determined by counting the extended SWNTs on the thermometers. Meanwhile, the background thermal conductance was measured on a micro device without

suspended SWNTs from the same batch-fabricated chip; this is because the micro thermometer devices from the same chip can be treated as identical given that they have gone through the same fabrication processes.

This manuscript was accepted by Appl. Phys. Lett. Click here to see the version of record.

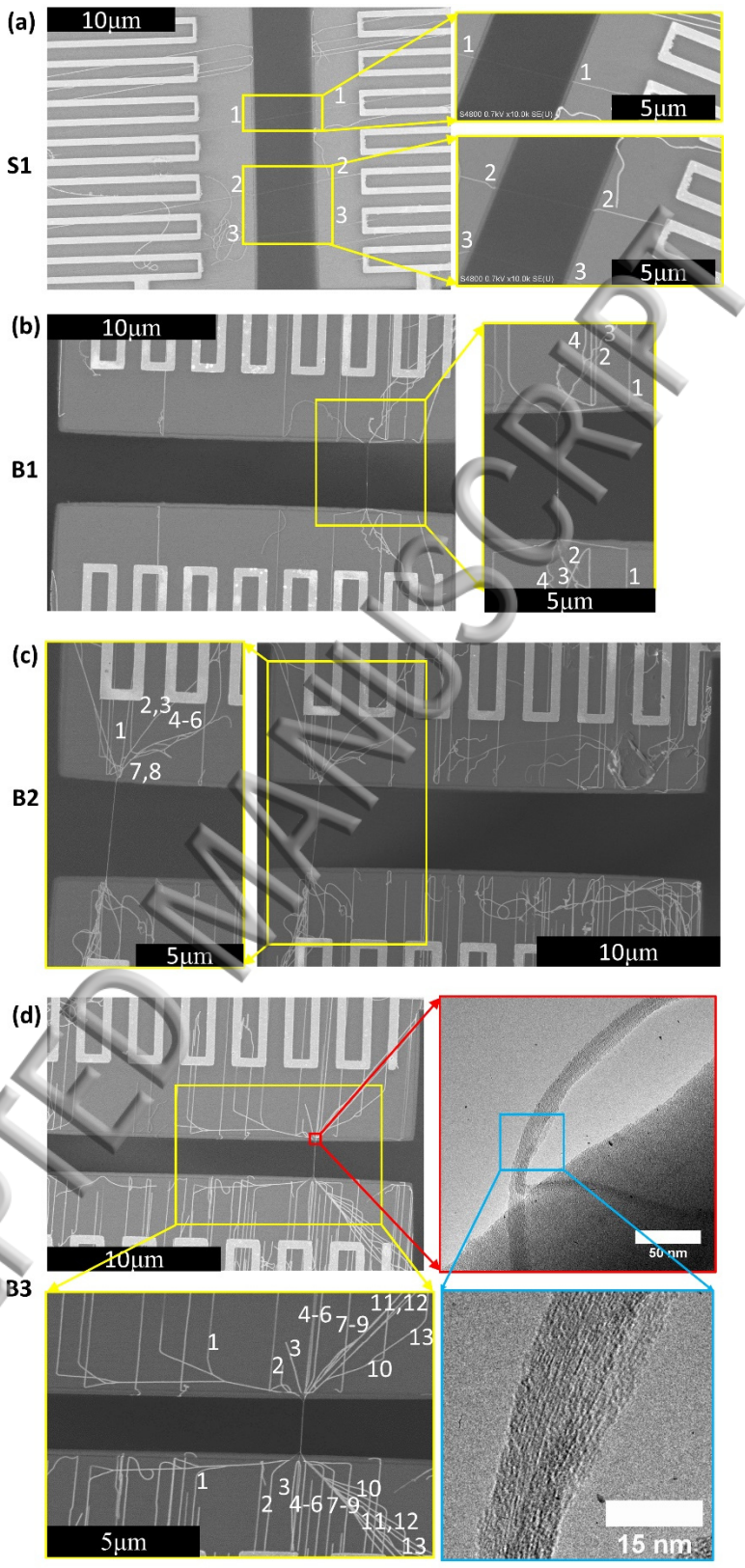

This manuscript was accepted by Appl. Phys. Lett. Click here to see the version of record.

Figure 1. SEM images of (a) sample S1, comprising three isolated SWNTs, gap between the two thermometers: 5 μm; (b) sample B2, which corresponds to a bundle of four SWNTs, gap between the two thermometers: 4.5 μm; (c) sample B3, a bundle of eight SWNTs, gap between the two thermometers: 5 μm; (d) sample B3, a bundle of thirteen SWNTs, gap between the two thermometers: 2.5 μm, the TEM images on the right side were taken at the edge after the SWNT bundle was broken during TEM handling. The rectangles and arrows indicate partial enlarged views, and the numbers point to the extended fractions of the SWNTs on both thermometers.

The SWNTs on suspended thermometers are shown in Figure 1. Four different SWNT samples, denoted as S1 shown in Figure 1(a) comprising three isolated SWNTs, B1 in Figure 1(b)) a four-SWNT bundle, B2 in Figure 1(c) an eight-SWNT bundle, and B3 in Figure 1(d) a thirteen-SWNT bundle were measured in the present work. The annealing after HA-SWNT transfer significantly enhanced the contacts between SWNTs and substrate, keeping the suspended parts of SWNTs fairly straight and the supported parts well-aligned and dispersed.

The thermal conductance measurements and sample identification in SEM and TEM were performed on the same isolated SWNTs or SWNT bundles across the two suspended micro thermometers as shown in Figure 1, and the method was originally invented by Shi *et al.*[6] Four SWNT samples and the background thermal conductance, were measured in the present work, as shown in Figure 2. The measured thermal conductance is increasing with temperature first and then saturates at around 300 K, in accordance with previous theoretical predictions[13, 14] and other experimental observations.[15, 16] Therefore, thermal conductance of SWNT samples is determined by $G_s = G_{s,m} - G_{bg}$, in which G_{bg} is the polynomial fitting of background thermal conductance at corresponding temperature, as the black solid line shows in Figure 2.

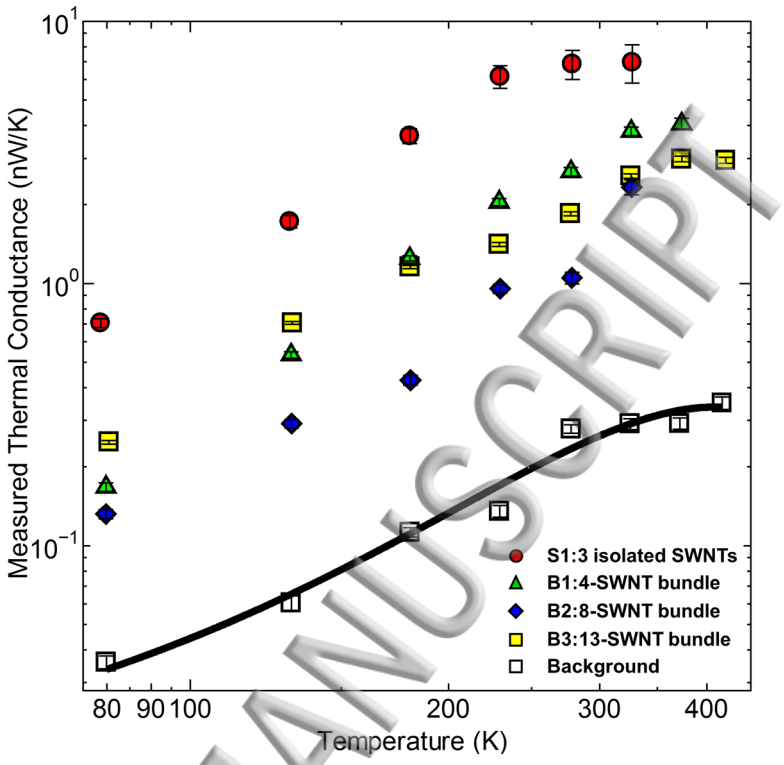

Figure 2. Measured thermal conductance of four SWNT samples, denoted as S1 (red dots), B1 (green triangles), B2 (blue rhombuses), and B3 (yellow squares), as well as the background thermal conductance (blank squares). The solid line is a polynomial fitting of the background thermal conductance.

To account for the TBR, interface thermal coupling per unit length ($g \approx 0.05 D \chi \left(\frac{T}{200}\right)^{1/3}$, $Wm^{-1}K^{-1}$) developed for CNT-SiO_2 interactions using molecular dynamics simulations that consider the lattice contributions to thermal transport[17, 18] was adopted; and this approximation is in good agreement with previous analyses and measurements.[19-21] Using the fin heat transfer model,[22, 23] the TBR can be calculated by $\mathrm{TBR} = \frac{1}{\sqrt{g\kappa A}\tanh\left(L_c\sqrt{\frac{g}{\kappa A}}\right)}$; κ is the thermal conductivity

This manuscript was accepted by Appl. Phys. Lett. Click here to see the version of record.

of SWNT, A the cross-sectional area of one SWNT and L_c the contact length is large enough to fully thermalized SWNT with supporting membrane.[24] The average diameter D of an SWNT is 1.8 nm (based on the diameter distribution on quartz growth from a previous study[12] and the TEM characterization in this study), and the strength of the van der Waals interaction χ is assumed to be 2. That was owing to significantly improved contacts by annealing after horizontally aligned SWNT transfer with PMMA in comparison with the direct growth of CNTs[25-27] on micro thermometers or CNT solution dropping,[6] so the SWNTs after PMMA decomposition were still well aligned on the membranes; the extended SWNTs of the bundles on the thermometers were still dispersed and the suspended parts were fairly straight, as shown in the SEM images in Figure 1. The results showed that TBR was two orders of magnitude lower than the measured total thermal resistance of S1 (less than 5% of the total thermal resistance), making the contact resistance in the present insignificant, so we ignored it in the later calculation of effective thermal conductivity with the uniform temperature distribution on the membranes.[28]

Sample S1 comprised three individual SWNTs across the 5 μm gap of the micro thermometer device, as shown in Figure 1, in which numbers 1 to 3 indicated the extended ends of the SWNTs on the thermometers. The three other SWNT samples evaluated in this study were B1, B2, and B3, which corresponded to SWNT bundles comprising four, eight, and thirteen SWNTs, respectively. There were tens of micrometers long transferred horizontally aligned SWNTs on both thermometers, keeping the suspended part very straight over the gap. After removing the background thermal conductance from the measured thermal conductance of the samples, the effective thermal conductivity of the samples was calculated as $\kappa = G_s \times L/A_s$, where L is the length of the suspended SWNTs and A_s is the cross-sectional area of the samples. The cross-sectional area of a sample was calculated as $n\pi\delta D$, where n is the number of SWNTs in the sample, δ equals

This manuscript was accepted by Appl. Phys. Lett. Click here to see the version of record.

0.34 nm[29] which corresponds to van der Waals thickness of monolayer graphene. Figure 3 shows the effective thermal conductivity κ obtained for the isolated SWNTs (S1) and the SWNT bundles (B1, B3, and B3).

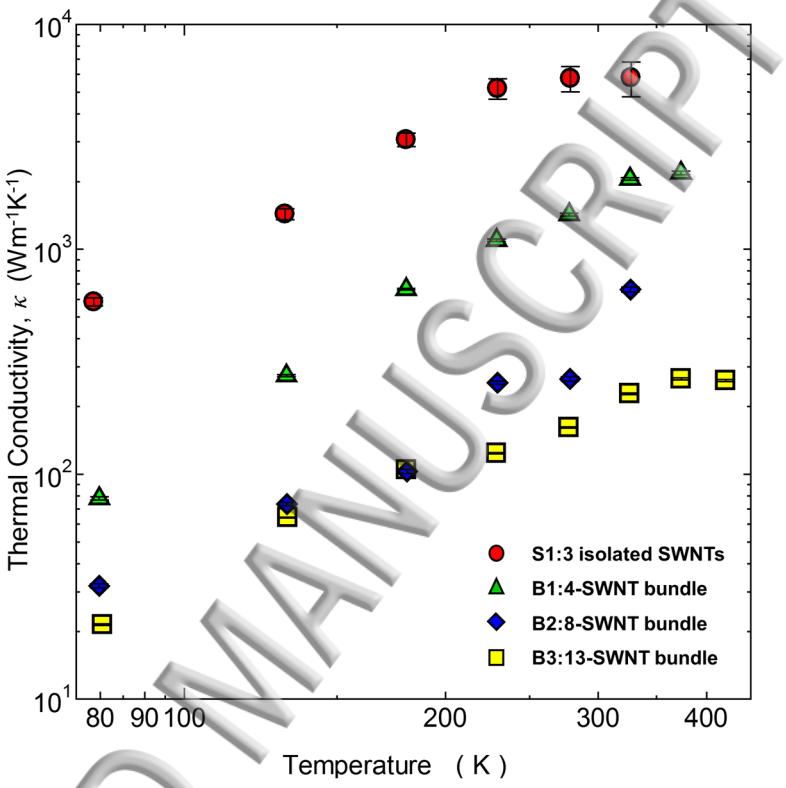

Figure 3. Effective thermal conductivity of S1 (red dots), B1 (green triangles), B2 (blue rhombuses), and B3 (yellow squares) as a function of temperature.

Initially, the thermal conductivity increases with temperature, after which it reaches to saturate around room temperature. The isolated SWNTs have the highest thermal conductivity, and this is in agreement with previous reports.[7, 16, 30] The thermal conductivity is much lower in the SWNT bundles, as indicated in Figure 3, and decreases with the increasing size of bundles. Besides, Figure 4 presents the effective thermal conductivity that logarithmically decreases with the increasing number of SWNTs in a bundle; however, it is at a decreasing rate. In consideration of the length

This manuscript was accepted by Appl. Phys. Lett. Click here to see the version of record.

dependency of thermal conductivity[31-33] and B3 is half of the length of the others, the decrease of thermal conductivity from B2 (eight-SWNT bundle) to B3 (thirteen-SWNT bundle) is inconspicuous. This degradation of thermal conductivity that results from the formation of bundles can be attributed to the inter-tube interactions that strongly increase phonon scatterings involving phonons from neighboring SWNTs,[34] and it has been observed in other experiments.[6, 7, 26, 35, 36] Shi *et al.*[6] measured that the thermal conductivity of 10 nm diameter SWNT bundle is two orders of magnitude larger than that of 148nm diameter bundle, and even one more order of magnitude larger in the isolated SWNT.[7] In the work of Hsu *et al.*,[26] the thermal conductivity of four-SWNT bundle can be several times larger than that of five-SWNT bundle with similar length.

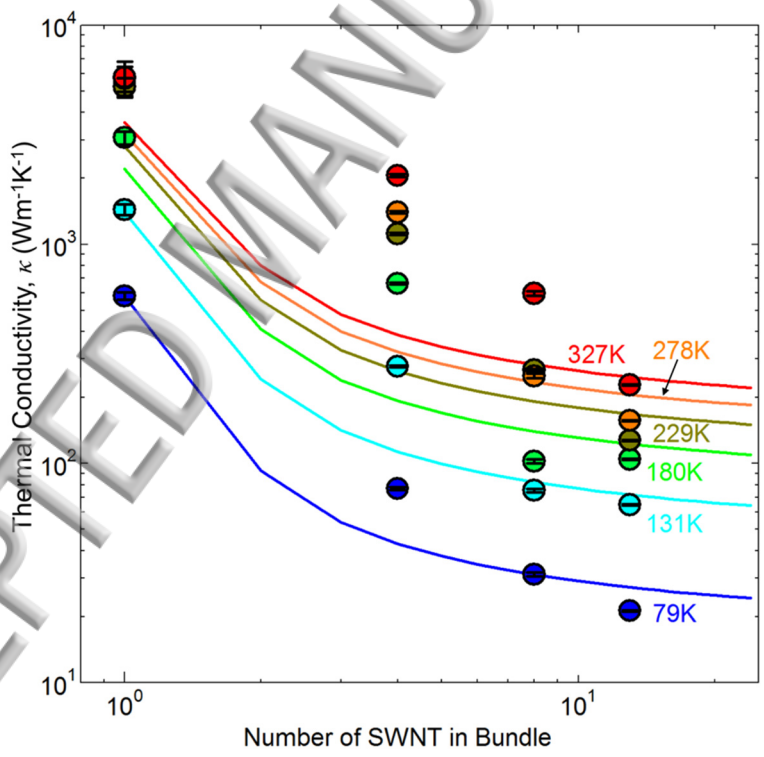

Figure 4. Effective thermal conductivity plotted against the number of SWNTs in a bundle at different temperatures (circles). The solid lines represent the fitting of the experimental data with

This manuscript was accepted by Appl. Phys. Lett. Click here to see the version of record.

the scattering rate through kinetic theory at corresponding temperatures (Blue @ 79 K; Cyan @ 131 K; Green @ 180 K; Brown @ 229 K; Orange @ 278 K; Red @ 327 K).

Within the frame work of kinetic theory,[37] the thermal conductivity in insulators or semiconductor materials can be expressed as $\kappa = \frac{1}{3}Cv^2\tau$, where C is the lattice volumetric specific heat, v is the average speed of the corresponding phonons, and τ is the relaxation time. Additionally, τ is the reciprocal of the scattering rate (γ) between phonons. For an isolated SWNT, its average scattering rate is γ_{is}, and the addition of N SWNTs increases the scattering rate by γ_{bu} (N), which is proportional to the increased number of interactions (n) per nanotube in the bundle.

$$\tau = \frac{1}{\gamma};\quad \gamma = \gamma_{is} + \gamma_{bu}(N)$$

$$\gamma_{bu}(N) \propto \text{Number of interactions per nanotube } (n/N)$$

Therefore, the thermal conductivity in SWNT bundle can be expressed as

$$\kappa = \frac{1}{3}Cv^2\frac{1}{\gamma_{is}+\gamma_{bu}(N)} = \frac{Cv^2}{3\gamma_{is}} \times \frac{1}{1+\frac{\gamma_{bu}(N)}{\gamma_{is}}} = \kappa_{is} \times \frac{1}{1+\sigma},$$

in which, $\kappa_{is} = \frac{Cv^2}{3\gamma_{is}}$ is thermal conductivity of isolated SWNT, along with $\sigma = \frac{\gamma_{bu}(N)}{\gamma_{is}}$ are parameters that are going to fit with the experimental data. The physical meaning of σ is the ratio of increased scatterings with neighboring SWNTs over the average scattering in an isolated SWNT; and the equation above indicates that with $\sigma = 1$, the thermal conductivity will reduce a half, while σ is much larger than 1 in SWNT bundles as shown in the following, leading to a serious deterioration in thermal conductivity as the experiments revealed.

This manuscript was accepted by Appl. Phys. Lett. Click here to see the version of record.

The thermal conductivity is inversely proportional to the phonon scattering rate; with the increase of bundle size, the probability of scatterings with the neighboring SWNTs increases, so that the thermal conductivity will decrease with more SWNTs in bundle. The experimental data was fitted with the equation above, as shown by the solid lines in Figure 4. Parameter κ_{is} can be referred to the measured value of isolated SWNT in this measurement, and the specific heat of carbon nanotubes increases with temperature indicated in a measurement with millimeter-long aligned multi-walled CNT over the temperature range of 10-300 K,[38] and the average group velocities of acoustic phonons that contribute the most to heat transfer hardly depend on temperature.[37] Furthermore, the scattering rate in an isolated SWNT γ_{is} increases with temperature due to the enhanced lattice vibration. Therefore, parameter κ_{is} has the same trend as the measured value with increasing temperature; parameter σ will decrease with temperature due to the increase of γ_{is} and that the temperature effect on γ_{bu} (N) has not been considered here, as presented in Figure 5. In this model, at around room temperature, thermal conductivity will be reduced to 1/10 by bundling with four SWNTs, 1/13 for eight-SWNT bundle, and 1/15 for thirteen-SWNT bundle. The decreasing rate of interactions between SWNTs with bundle size is also obvious in Figure 5(b).

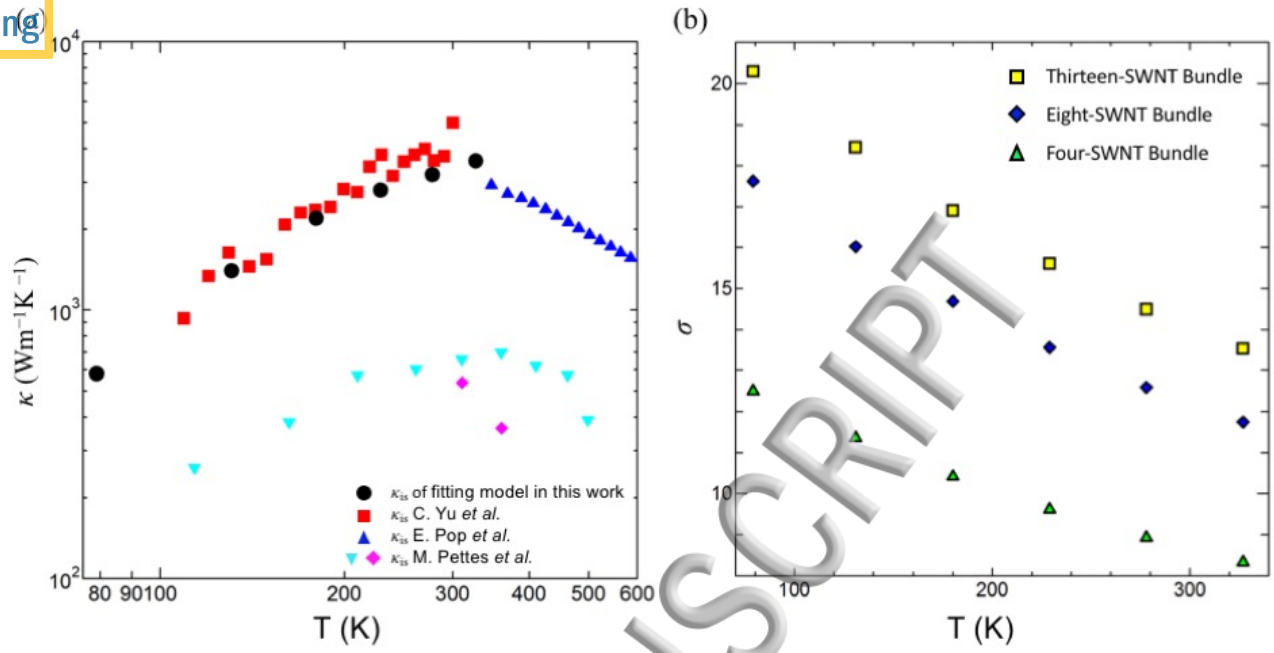

Figure 5. Temperature dependency of fitting parameters (a) κ_{is} in black dots and thermal conductivity of isolated SWNT from previous measurements; (b) σ: the green triangle is fitted with four-SWNT bundle, the blue rhombuses with eight-SWNT bundle, and the yellow squares with thirteen-SWNT bundle.

The fitting curves deduced from the kinetic theory above are in the same trend with the measurements shown in Figure 4, indicating that the interactions with neighboring SWNTs is inelastic scattering that strongly quenches the phonon modes in the SWNTs leading to the very low thermal conductivity of bundled SWNTs. Therefore, the interactions between SWNTs are probably much stronger or more complex than that predicted by previous studies.[8, 39] It has been reported that the superior thermal conductivity in monolayer graphene[40] is worsened by being in contact with a substrate,[4] due to the phonon leaking across the interface and strong suppressing of flexural modes by interfacial scattering. A recent report[37] reveals that encapsulated fullerene greatly impedes the thermal transport in SWNTs because of a slight radial expansion of the

This manuscript was accepted by Appl. Phys. Lett. Click here to see the version of record.

nanotube caused by the fullerene. Similarly, the interactions between SWNTs might cause certain deformations in the isolated SWNTs that lead to a decrease in thermal conductivity in the bundles.

The structure dependency of thermal conductivity is necessary for the design of SWNT electronics regarding to the stability and durability of its performance, and the findings in this study provide fresh insights to determine it experimentally. With the transferred HA-SWNTs on micro thermometer device, the size of a bundle can be selectively determined allowing for a quantitative evaluation of the effect of bundle size on the thermal conductivity of SWNTs. On account of the large overlapped areas of the SWNTs and supporting thermometers, the TBR greatly decreases and it becomes negligible while calculating the effective thermal conductivity of the SWNTs. The obtained thermal conductivity was the highest for the sample with three isolated SWNTs, approximately $5000\pm1000 Wm^{-1}K^{-1}$. The bundles exhibit a much lower thermal conductivity that decreases with the bundle size. The logarithmical deterioration of thermal conductivity in the bundles can be attributed to the increased scattering rate with neighboring SWNTs that impedes the phonon transport of isolated SWNTs. These results are explained by an empirical analysis based on the kinetic theory, indicating that the interactions between SWNTs might be much stronger than that predicted in previous studies.

SUPPLEMENTARY MATERIAL

Details about growth of HA-SWNT, fabrication of micro thermometers with transferred HA-SWNT, bundle size characterization, thermal boundary resistance, thermal conductance measurements, and number of interactions between SWNTs in bundles are available in Supporting

Information of Quantitative study of bundle size effect on thermal conductivity of single-walled carbon nanotubes.

ACKNOWLEDGMENTS

Part of this work was financially supported by JSPS KAKENHI Grant Numbers JP15H05760, JP25107002, JP17K06187, and JP17K14601. Part of this work was supported by the "Nanotechnology Platform Japan" of the Ministry of Education, Culture, Sports, Science and Technology (MEXT), in Takeda Cleanroom with the help of the Nanofabrication Platform Center of the VLSI Design and Education Center (VDEC), the University of Tokyo, Japan

REFERENCES

1. K. Otsuka, T. Inoue, E. Maeda, R. Kometani, S. Chiashi, S. Maruyama, ACS Nano **11,** 11497 (2017).

2. M. Steiner, M. Freitag, V. Perebeinos, J. C. Tsang, J. P. Small, M. Kinoshita, D. Yuan, J. Liu, P. Avouris, Nature Nanotech. **4**, 320 (2009).

3. S. Chen, A. L. Moore, W. Cai, J. W. Suk, J. An, C. Mishra, C. Amos, C. W. Magnuson, J. Kang, L. Shi, ACS Nano **5**, 321 (2011).

4. J. H. Seol, I. Jo, A. L. Moore, L. Lindsay, Z. H. Aitken, M. T. Pettes, X. Li, Z. Yao, R. Huang, D. Broido, Science **328**, 213 (2010).

5. S. Ghosh, W. Bao, D. L. Nika, S. Subrina, E. P. Pokatilov, C. N. Lau, A. A. Balandin, Nature Mater. **9**, 7 (2010).

6. L. Shi, D. Li, C. Yu, W. Jang, D. Kim, Z. Yao, P. Kim, A. Majumdar, J Heat Trans. **125**, 881 (2003).

7. C. Yu, L. Shi, Z. Yao, D. Li, A. Majumdar, Nano Lett. **5**, 1842 (2005).

8. A. N. Volkov, R. N. Salaway, L. V. Zhigilei, J Appl. Phys. **114**, 104301 (2013).

9. T. Inoue, D. Hasegawa, S. Badar, S. Aikawa, S. Chiashi, S. Maruyama, J Phys. Chem. C **117**, 11804 (2013).

10. L. Jiao, B. Fan, X. Xian, Z. Wu, J. Zhang, Z. Liu, J Am. Chem. Soc. **130**, 12612 (2008).

11. J. Wang, Z. Jin, J. Cheng, Y. Li, J Phys. Chem. C, **113**, 8132 (2009).

12. H. Ago, N. Uehara, K.-I. Ikeda, R. Ohdo, K. Nakamura, M. Tsuji, Chem. Phys. Lett. **421**, 399 (2006).

13. M. A. Osman, D. Srivastava, Nanotechnology **12**, 21 (2001).

14. J. R. Lukes, H. Zhong, J Heat Trans. **129**, 705 (2007).

15. P. Kim, L. Shi, A. Majumdar, P. McEuen, Phys. Rev. Lett. **87**, 215502 (2001).

16. E. Pop, D. Mann, Q. Wang, K. Goodson, H. Dai, Nano Lett. **6**, 96 (2006).

17. Z.-Y. Ong, E. Pop, Phys. Rev. B, **81**, 155408 (2010).

18. K. Otsuka, T. Inoue, Y. Shimomura, S. Chiashi, S. Maruyama, Nano Res. **10**, 3248 (2017).

19. R. Prasher, Phys. Rev. B **77**, 075424 (2008).

20. L. Shi, J. Zhou, P. Kim, A. Bachtold, A. Majumdar, P. L. McEuen, J Appl. Phys. **105**, 104306 (2009).

21. E. Pop, D. A. Mann, K. E. Goodson, H. Dai, J Appl. Phys. **101**, 093710 (2007).

22. A. Weathers, L. Shi, Annu. Rev. Heat Trans. **16**, 40 (2013)

23. I. Jo, M. T. Pettes, L. Lindsay, E. Ou, A. Weathers, A. L. Moore, Z. Yao, L. Shi, AIP Adv. **5**, 053206 (2015)

24. J. Yang, Y. Yang, S. W. Waltermire, T. Gutu, A. A. Zinn, T. T. Xu, Y. Chen, D. Li, Small **7**, 16 (2011)

25. M. T. Pettes, L. Shi, Adv. Funct. Mater. **19**, 3918 (2009).

26. I.-K. Hsu, M. T. Pettes, A. Bushmaker, M. Aykol, L. Shi, S. B. Cronin, Nano Lett. **9**, 590 (2009).

27. I.-K. Hsu, M. T. Pettes, M. Aykol, L. Shi, S. B. Cronin, J Appl. Phys. **108**, 084307 (2010).

28. A. L. Moore, L. Shi, Meas. Sci. Technol. **22**, 015103 (2010).

29. S. Maruyama, Microscale Therm. Eng. **7**, 41 (2003).

30. S. Berber, Y. K. Kwon, D. Tománek, Phys. Rev. Lett. **84**, 4613 (2000).

31. S. Maruyama, Physica B, **323**, 193 (2002).

32. V. Lee, C.-H. Wu, Z.-X. Lou, W.-L. Lee, C.-W. Chang, Phys. Rev. Lett. **118**, 135901 (2017).

33. A. M. Marconnet, M. A. Panzer, K. E. Goodson, Rev. Mod. Phys. **85**, 1295 (2013)

34. J. Cao, X. Yan, Y. Xiao, J. Ding, Phys. Rev. B **69**, 073407 (2004).

35. I.-K. Hsu,;R. Kumar, A. Bushmaker, S. B. Cronin, M. T. Pettes, L. Shi, T. Brintlinger, M. S. Fuhrer, J. Cumings, Appl. Phys. Lett. **92**, 63119 (2008).

36. T. Kodama, M. Ohnishi, W. Park, T. Shiga, J. Park, T. Shimada, H. Shinohara, J. Shiomi, K. E. Goodson, Nature Mater. **16**, 892 (2017).

37. Z. M. Zhang, Nano/Microscale Heat Transfer, pp 162 (2007).

38. W. Yi, L. Lu, D.-L. Zhang, Z. Pan, S. Xie, Phys. Rev. B **59**, R9015 (1999).

39. J. Hone, B. Batlogg, Z. Benes, A. Johnson, J. Fischer, Science **289**, 1730 (2000).

40. A. A. Balandin, S. Ghosh, W. Bao, I. Calizo, D. Teweldebrhan, F. Miao, C. N. Lau, Nano Lett. **8**, 3 (2008)

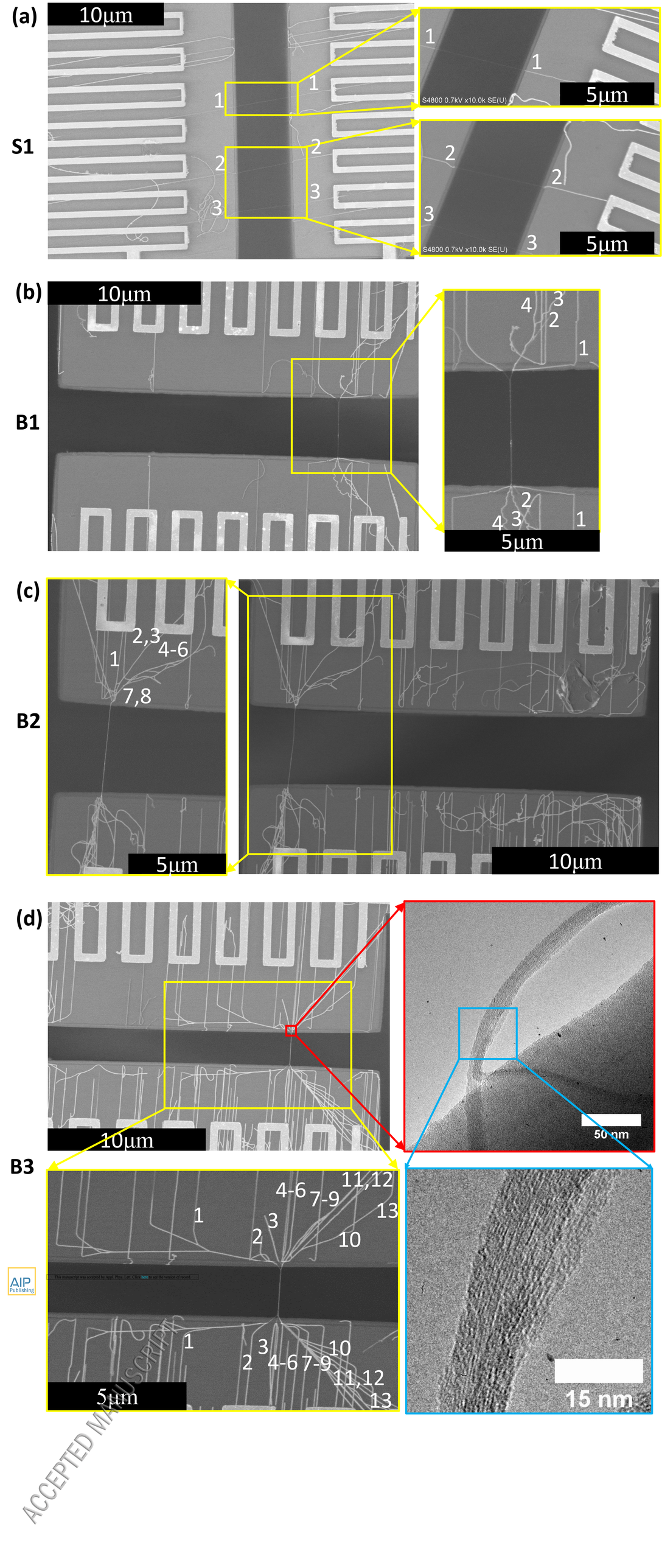

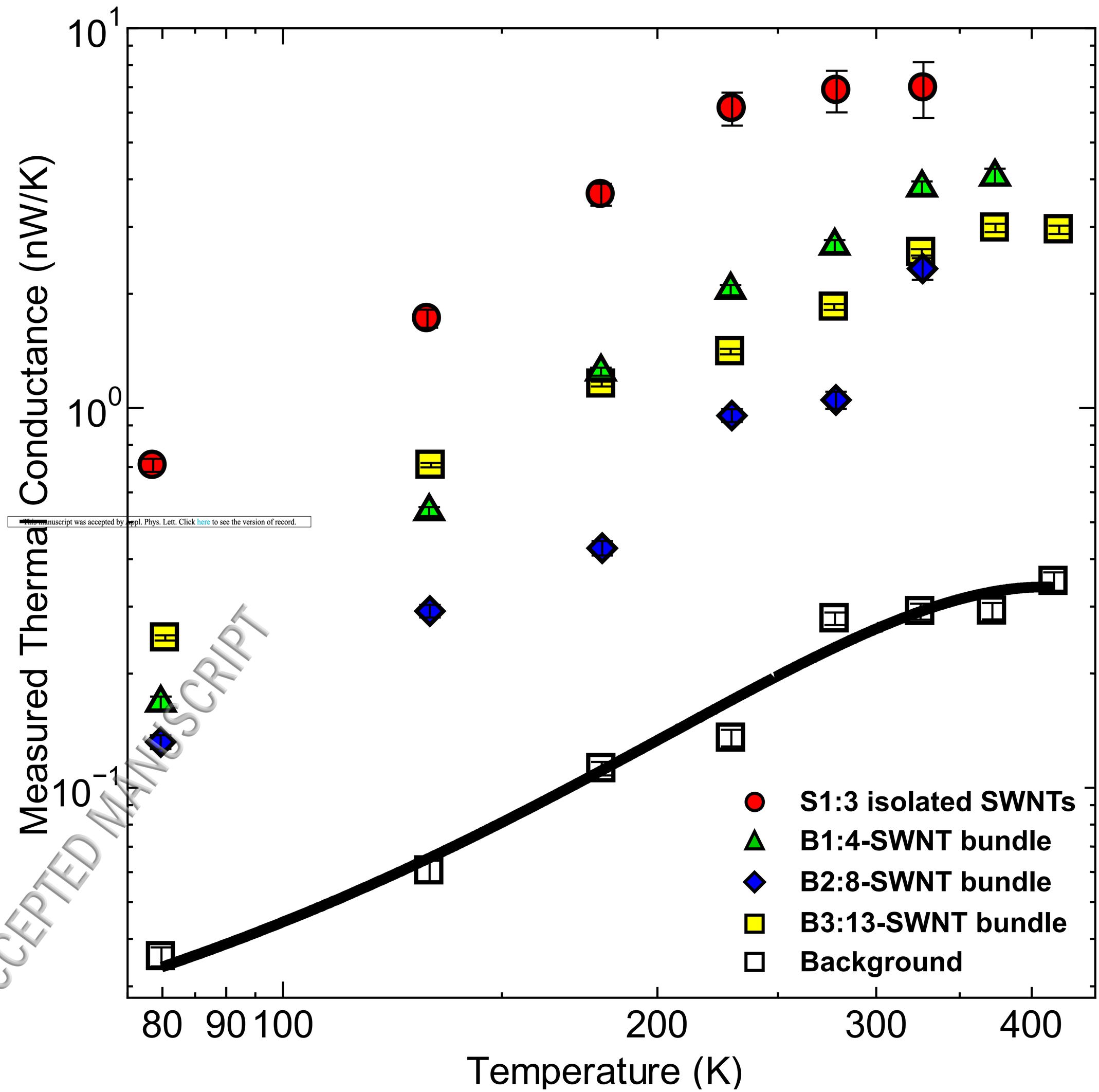

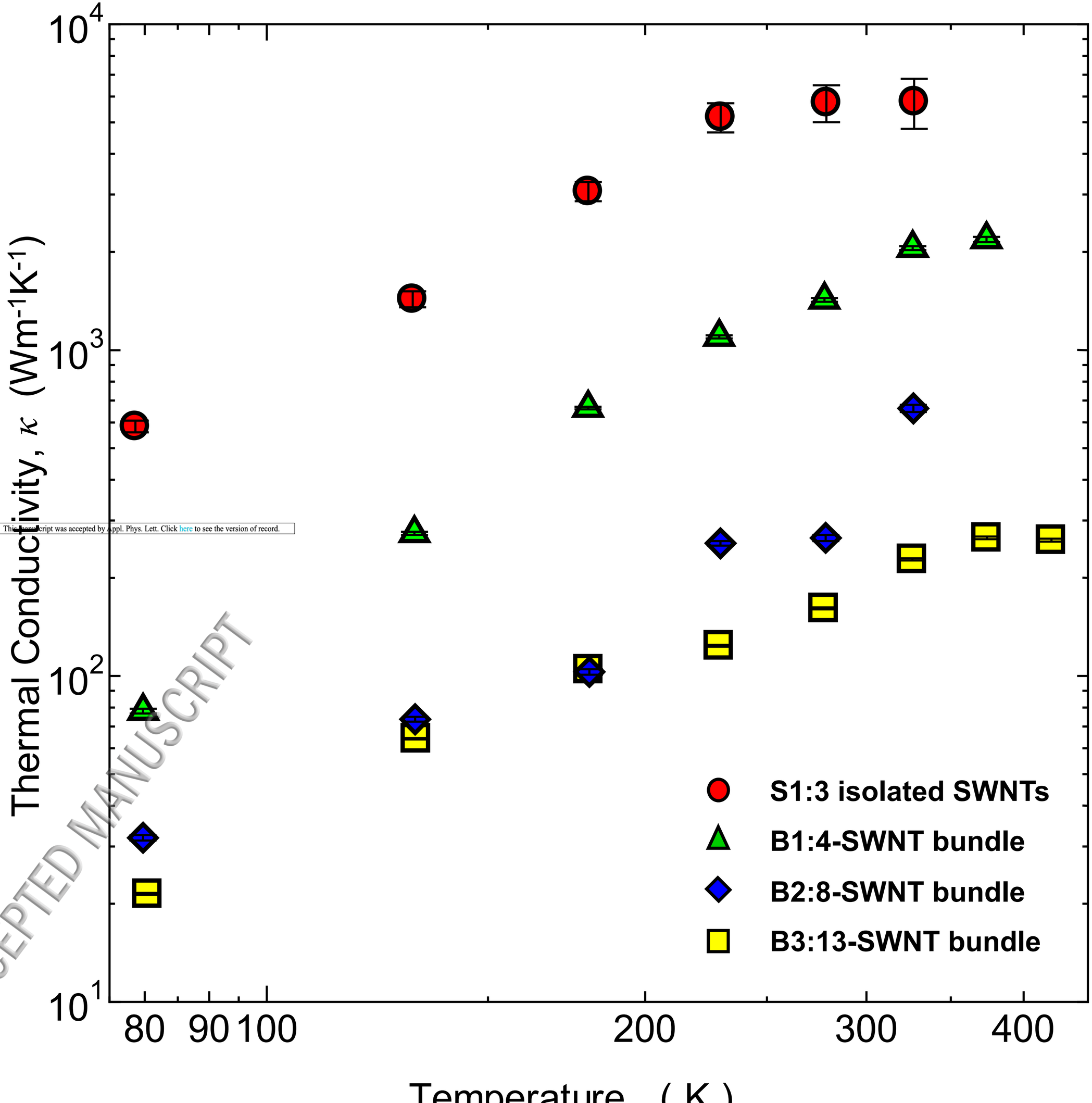

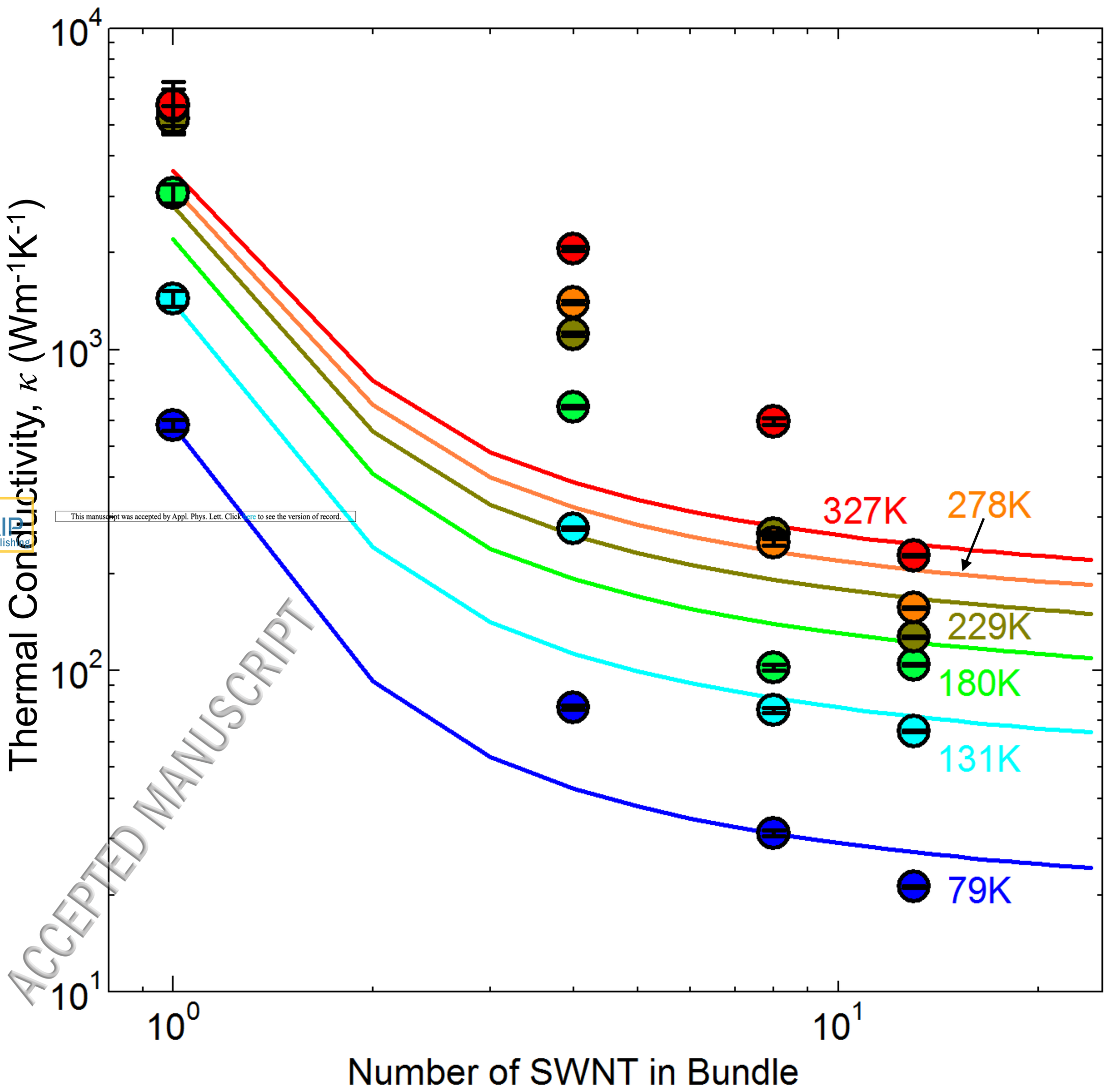

(a)

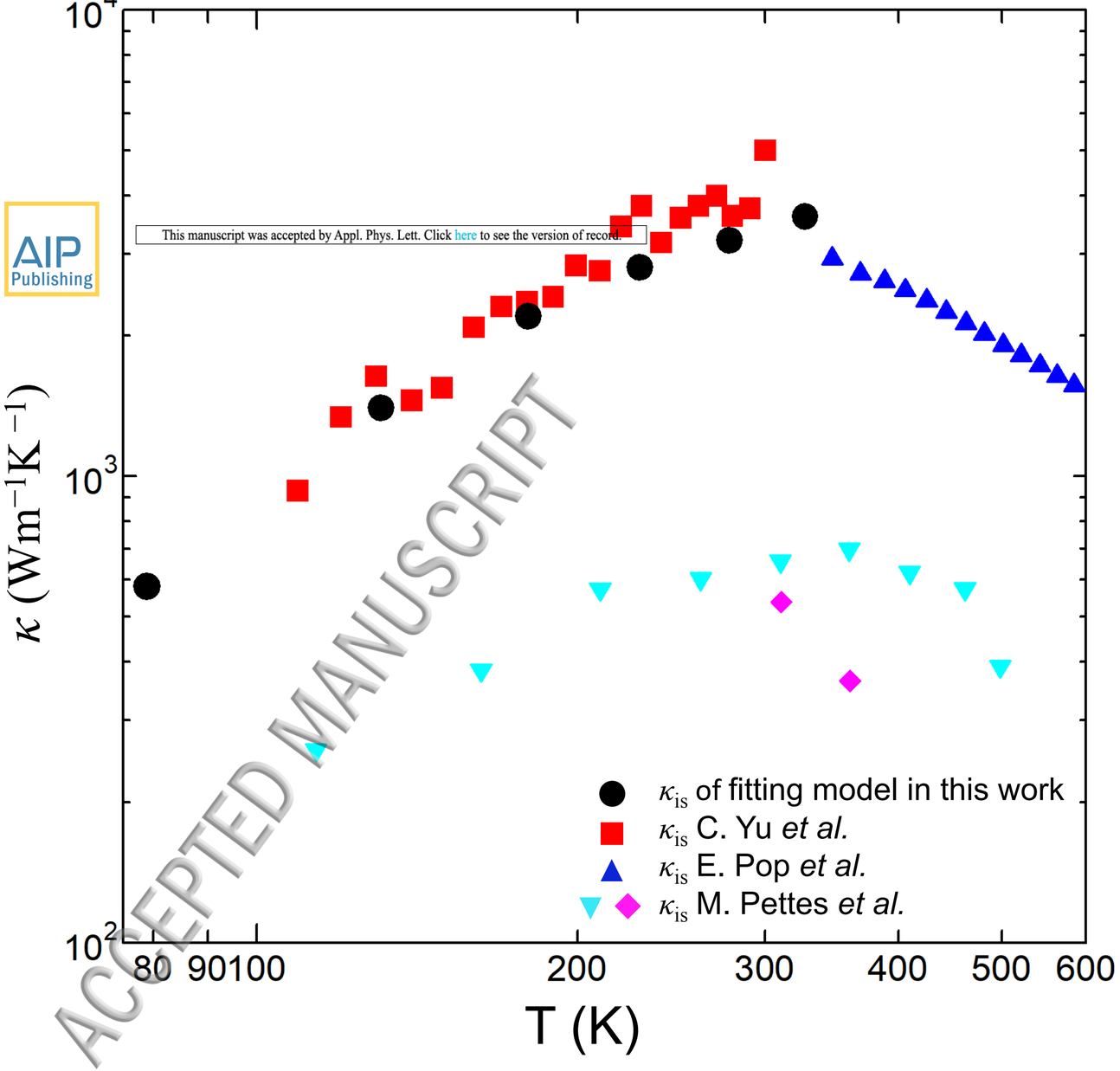

(b)